

Comparative assessment of nitrogen fixation rate by $^{15}\text{N}_2$ tracer assays in the South China Sea

Danyang Li^{1,2}, Minfang Zheng¹, Yusheng Qiu¹, Limin Lai^{3,4}, Nengwang Chen^{3,4}, Hongmei Jing⁵, Run Zhang^{1*}, Min Chen¹

¹ College of Ocean and Earth Sciences, Xiamen University, Xiamen 361102, China

² Fisheries College, Jimei University, Xiamen 361021, China

³ College of the Environment and Ecology, Xiamen University, Xiamen 361102, China

⁴ State Key Laboratory of Marine Environment Science, Xiamen University, Xiamen 361102, China

⁵ Key Laboratory for Experimental Study under Deep-sea Extreme Conditions, Institutes of Deep-sea Science and Engineering, Chinese Academy of Sciences, Sanya 572000, China

Received 13 January 2022; accepted 18 March 2022

© Chinese Society for Oceanography and Springer-Verlag GmbH Germany, part of Springer Nature 2023

Abstract

Nitrogen fixation is one of the most important sources of new nitrogen in the ocean and thus profoundly affects the nitrogen and carbon biogeochemical processes. The distribution, controlling factors, and flux of N_2 fixation in the global ocean remain uncertain, partly because of the lack of methodological uniformity. The $^{15}\text{N}_2$ tracer assay (the original bubble method \rightarrow the $^{15}\text{N}_2$ -enriched seawater method \rightarrow the modified bubble method) is the mainstream method for field measurements of N_2 fixation rates (NFRs), among which the original bubble method is the most frequently used. However, accumulating evidence has suggested an underestimation of NFRs when using this method. To improve the availability of previous data, we compared NFRs measured by three $^{15}\text{N}_2$ tracer assays in the South China Sea. Our results indicate that the relationship between NFRs measured by the original bubble method and the $^{15}\text{N}_2$ -enriched seawater method varies obviously with area and season, which may be influenced by incubation time, diazotrophic composition, and environmental factors. In comparison, the relationship between NFRs measured by the original bubble method and the modified bubble method is more stable, indicating that the N_2 fixation rates based on the original bubble methods may be underestimated by approximately 50%. Based on this result, we revised the flux of N_2 fixation in the South China Sea to 40 $\text{mmol}/(\text{m}^2\cdot\text{a})$. Our results improve the availability and comparability of literature NFR data in the South China Sea. The comparison of the $^{15}\text{N}_2$ tracer assay for NFRs measurements on a larger scale is urgently necessary over the global ocean for a more robust understanding of the role of N_2 fixation in the marine nitrogen cycle.

Key words: N_2 fixation rate, South China Sea, $^{15}\text{N}_2$ tracer assay

Citation: Li Danyang, Zheng Minfang, Qiu Yusheng, Lai Limin, Chen Nengwang, Jing Hongmei, Zhang Run, Chen Min. 2023. Comparative assessment of nitrogen fixation rate by $^{15}\text{N}_2$ tracer assays in the South China Sea. *Acta Oceanologica Sinica*, 42(1): 75–82, doi: 10.1007/s13131-022-2092-3

1 Introduction

N_2 fixation, the biological reduction of N_2 gas to ammonium, is a dominant source of reactive nitrogen in marine environments (Gruber and Sarmiento, 1997; Codispoti, 2007), thus playing a key role in carbon and nitrogen biogeochemical cycles and exerting a profound impact on global climate (Casciotti, 2016; Zehr and Capone, 2020). In the context of global warming, many efforts have been made to obtain the distribution of the N_2 fixation rates (NFRs) (Zehr and Capone, 2020). However, relatively large uncertainties remain because of the lack of methodological uniformity (White et al., 2020; Zehr and Capone, 2020). The most common method used to measure marine NFRs has been the $^{15}\text{N}_2$ tracer assay, which traces the incorporation of isotope labeled N_2 gas ($^{15}\text{N}_2$) into the particulate matter. This method was first applied to the field measurement of marine NFRs in the Sargasso Sea (Dugdale et al., 1961) and has been optimized and

widely applied since then (Montoya et al., 1996; Mohr et al., 2010; Klawonn et al., 2015), generating a large body of field NFR data in the global ocean (White et al., 2020).

According to the introduction of the $^{15}\text{N}_2$ tracer to the incubation system, the present $^{15}\text{N}_2$ tracer assay for NFRs measurements can be classified into the original bubble method (B method hereafter) (Montoya et al., 1996), the $^{15}\text{N}_2$ -enriched seawater method (S method hereafter) (Mohr et al., 2010), and the modified bubble method (MB method hereafter) (Chang et al., 2019; Klawonn et al., 2015). The B method was first described in detail by Montoya et al. (1996). In brief, the $^{15}\text{N}_2$ tracer can be introduced into the incubation system by injecting an aliquot of $^{15}\text{N}_2$ gas to facilitate a dissolution equilibrium of the $^{15}\text{N}_2$ gas bubble. After incubation (typically 6–24 h), the particulate material is captured by a glass fiber filter for later analyses of the mass and ^{15}N atom abundance of particulate N on an elemental analyzer

Foundation item: The National Natural Science Foundation of China under contract Nos 42076042 and 41721005; the Fund of Ministry of Science and Technology of China under contract No. 2017FY201403; the Fund of China Ocean Mineral Resources R&D Association under contract No. DY135-13-E2-03.

*Corresponding author, E-mail: zhangrun@xmu.edu.cn

coupled to an isotope ratio mass spectrometer. NFRs can be calculated using the equations in Montoya et al. (1996). Due to its relative simplicity, high precision, and sensitivity of the B method, it has been widely applied and has contributed to the main body of field NFRs data in the global ocean. However, the equilibration of labeled $^{15}\text{N}_2$ gas is relatively slow and largely depends on the incubation time. This raises the concern that the calculated initial atom abundance of the N_2 source pool (A_{N_2} , based on gas solubility laws) may be overestimated, resulting in the underestimation of NFRs (Böttjer et al., 2017; Montoya et al., 1996; Großkopf et al., 2012; Wilson et al., 2012). Accordingly, the S method was proposed (Mohr et al., 2010). The key modification that differentiates the S method from the B method is the introduction of $^{15}\text{N}_2$ -enriched seawater rather than the $^{15}\text{N}_2$ bubble into the incubation bottle (Mohr et al., 2010). The filtered seawater enriched with $^{15}\text{N}_2$ gas was added to a target $A_{\text{N}_2} \geq 5\%$, with an inoculum addition that was approximately 5% of the total incubation volume. Additionally, protocols have been developed to further optimize the $^{15}\text{N}_2$ tracer assay for NFRs, including removing the bioavailable ^{15}N -contaminants (such as $^{15}\text{NO}_x$) in commercial $^{15}\text{N}_2$ gas (Dabundo et al., 2014; Chen et al., 2018) and reducing the pore size (from 0.7 μm to 0.3 μm) of membranes for the collection of particulate nitrogen (Bombar et al., 2018).

In addition to the B and S methods, in recent five years, the MB method has been employed (Klawonn et al., 2015; Chang et al., 2019). Briefly, $^{15}\text{N}_2$ gas was added to the incubation bottle and mixed gently for ≤ 15 min before the gas bubble was displaced with unenriched water. Before filtration at the end of the incubation period, subsamples were collected to quantify the ^{15}N atom abundance of the dissolved $^{15}\text{N}_2$ gas in each incubation by using Member Inlet Mass Spectrometer (MIMS) or Isotope Ratio Mass Spectrometer (IRMS). Because A_{N_2} is directly measured, the MB method largely overcomes the underestimation of NFRs caused by the non-equilibration of $^{15}\text{N}_2$ gas and may also provide a relatively higher A_{N_2} (approximately 7–9 atom abundance; Chen et al., 2018) than the S method. Although the S and MB methods have been indicated to be more feasible for the field measurements of NFRs and have been gradually promoted in recent years (Großkopf et al., 2012; Wilson et al., 2012; Zhang et al., 2015, 2019; Gradoville et al., 2017), the comparison of field NFRs measured by the B, S, and MB methods has rarely been conducted (White et al., 2020). As most published NFRs are based on the B method and probably represent underestimates, there is an urgent need to provide scientific base for the potential correction of the large body of reported field NFR dataset with respect to methodology inconsistency (White et al., 2020; references therein).

The South China Sea (SCS) is the largest marginal sea in the western Pacific, with a surface area of approximately 3.5×10^6 km² (Chen et al., 2014). It provides an ideal site for comparing NFRs measured by the B, S, and MB methods, and the main reasons for this are as follows: (1) the SCS has wide continental shelves and a deep basin with a depth of approximately 4 700 m, causing obvious variation in the environmental characteristics and diazotrophic compositions in the SCS (Shiozaki et al., 2014), which may help reveal the influence of environmental factors and diazotrophic composition on the discrepancy of NFRs measured by the B, S, and MB methods; and (2) field NFR measurements in the SCS have been widely reported (Voss et al., 2006; Chen et al., 2008, 2014; Grosse et al., 2010; Li and Zhang, 2018), most of which were based on the B method, indicating the possible need for the correction of historical data. In this study, we aim to observe the discrepancy between NFRs based on the B, S, and MB methods and reveal the possible influences on their correlations,

improving the availability of the present NFRs in the SCS and re-evaluating the flux of N_2 fixation in the SCS. Our results may improve the understanding of global N_2 fixation and oceanic N budget.

2 Methods and materials

2.1 Sampling areas

Nine cruises were conducted between 2013 and 2018 (August 2013, July 2014, March and July 2017, and June 2018) in the open area of the SCS and the coastal Daya Bay (July 2015, December 2015, April 2016, and January 2018) in the northern SCS (Fig. 1). During the cruises from 2013 to 2016, NFRs measured by the B and S methods were compared. In March 2017 and July 2017, the large-scale determination of NFRs by the S method was conducted in the open areas of the SCS (Fig. 1a), and samples for nitrogenase gene (*nifH*) analysis were also collected in March 2017 (Fig. 1a). In January and June 2018, NFRs observed by the B and MB methods were compared. A part of NFR data in the Daya Bay can be found elsewhere (Li et al., 2019).

2.2 N_2 fixation rate

The $^{15}\text{N}_2$ gas (98% atom ^{15}N) used in this study was obtained from Cambridge Isotope Laboratories Inc., USA. A simplified purifying pathway ($^{15}\text{N}_2$ gas stock cylinder \rightarrow degassed sulfuric acid trap \rightarrow potassium permanganate trap) was applied to efficiently remove any possible residual contamination of the ^{15}N labeled fixed N (possibly nitrate and ammonium) described by Dabundo et al. (2014). Seawater samples were collected in Niskin bottles. Duplicate samples were collected and filled bubble-free into pre-cleaned (soaked in 0.1 mol/L HCl for 24 h and washed with Milli-Q water) clear 1.2 L Nalgene polycarbonate bottles. For samples measured by the B method, purified $^{15}\text{N}_2$ gas was immediately injected into the incubation system (2 mL/L). For samples measured by the S method, approximately 40 mL of the prepared ^{15}N -enriched seawater (10 mL of purified $^{15}\text{N}_2$ gas \rightarrow 1 L of pre-filtered degassed seawater) was added to the incubation bottles. For samples measured by the MB method, purified $^{15}\text{N}_2$ gas was added to the incubation system and then shaken until bubbles disappeared, duplicate subsamples (approximately 12.5 mL) were collected to observe the ^{15}N abundance in the incubation system, and the incubation bottles were refilled before incubation. Samples collected from the Daya Bay and the open areas of the SCS were incubated for 6 h and 24 h, respectively.

After incubation, NFR samples were filtered onto pre-combusted (450 °C, 4 h) glass fiber filter membranes (GF-75). The membranes were then dried at 60 °C and stored at -20 °C until measurement. Natural suspended particulate organic matter samples were also collected for background ^{15}N analysis by filtering 4 L of seawater onto the filters. Particulate nitrogen and ^{15}N abundance ($\delta^{15}\text{N}$ vs. air N_2) were measured by EA (Carlo Erba NC 2500)-IRMS (Finnigan Delta V Advantage). The reproducibility of $\delta^{15}\text{N}$ measurements was smaller than 0.2‰. NFR was calculated using the equations described by Montoya et al. (1996). The minimum quantifiable rate (MQR) of NFRs was also calculated after error propagation (Montoya et al., 1996; Gradoville et al., 2017). Measured NFRs below the MQR were considered undetectable (n.d.). Only validated values were used for the interpretation.

2.3 Analysis of *nifH*

Samples for *nifH* gene analysis were collected at seven stations (Fig. 1a) in March 2017 by filtering approximately 2 L of seawater onto Millipore polycarbonate filters (pore size 0.2 μm) and

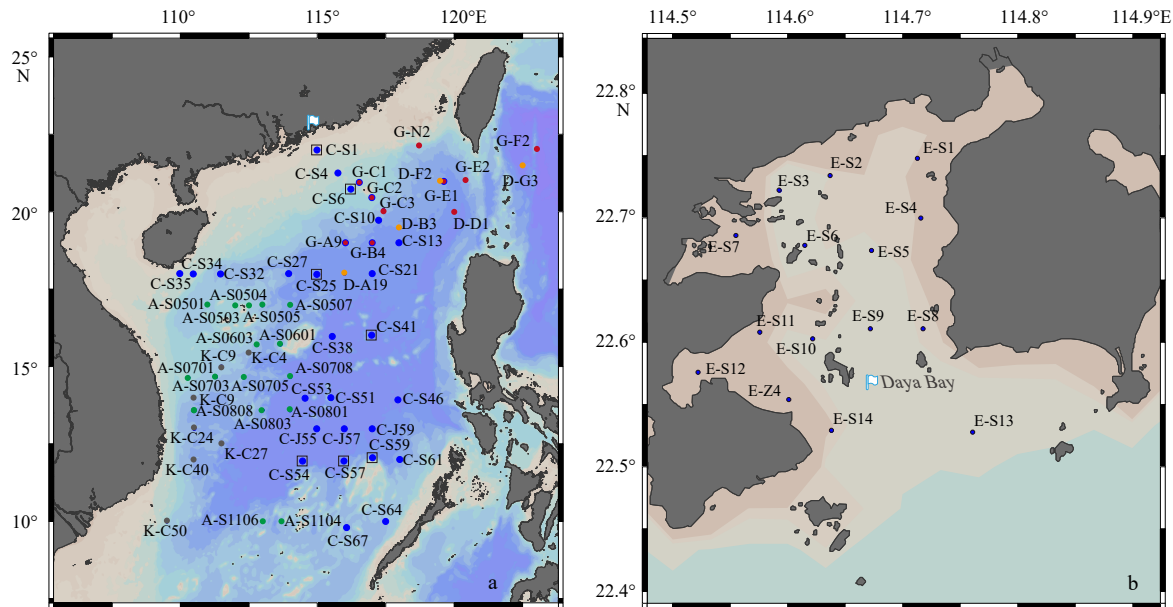


Fig. 1. Sampling locations in the South China Sea (SCS): a. stations in the open areas of the SCS from 2013 to 2017 (“A-”, “K-”, “C-”, “G-” and “D-” indicate cruises in August 2013, July 2014, March 2017, July 2017 and June 2018, “□” indicates the sampling stations of *nifH* in March 2017); b. stations in the Daya Bay (prefixed with “E-”, July 2015, December 2015, April 2016 and January 2018).

then stored in liquid nitrogen until analysis. In the laboratory, the filters were cut into small pieces, and genomic DNA was extracted using a Qiagen DNeasy plant extraction kit by following the manufacturer’s instructions. *NifH* gene fragments of approximately 360 bp were amplified using nested PCR (Zehr and Turner, 2001; Zehr et al., 2007). Barcodes were incorporated with primers to enable sample multiplexing during sequencing. Paired-end sequencing of the amplicons was performed using an Illumina MiSeq sequencer (Novogene Co., Ltd., www.novogene.com).

The sequences generated in this study were processed using Mothur software (Schloss, 2009). Barcodes and primer sequences were trimmed, and chimeric sequences were identified. Reads less than 310 bp in length and sequences with undetermined nucleotides were removed. The remaining sequences were translated into amino acid sequences using Ribosomal Database Project Framebot and then aligned against the *nifH* ref-seqs database from National Center for Biotechnology Information (<http://www.ncbi.nlm.nih.gov>). Sequences showing less than 80% similarity with the reference database were removed. In the remaining sequences, operational taxonomic units (OTUs) were defined with 95% sequence similarity as the cutoff value (Kong et al., 2011; Osorio-Santos et al., 2014). To identify the phylogenetic affiliation of the *nifH* sequences, the 50 most abundant OTUs and selected reference sequences from different diazotrophic groups were used to construct a neighbor-joining tree by using Molecular Evolutionary Genetics Analysis software. All sequences generated in this study have been submitted to the NCBI Sequence Read Archive (<http://www.ncbi.nlm.nih.gov/Traces/sra>, SRP 181068).

3 Results

3.1 NFRs

NFRs in the SCS open waters ranged from n.d. to 0.90 nmol/(L·d) during the sampling cruises (Fig. 2). The highest average NFR was observed in June 2018 (MB method), and the lowest value was observed in March 2017 (S method). In August 2013, surface

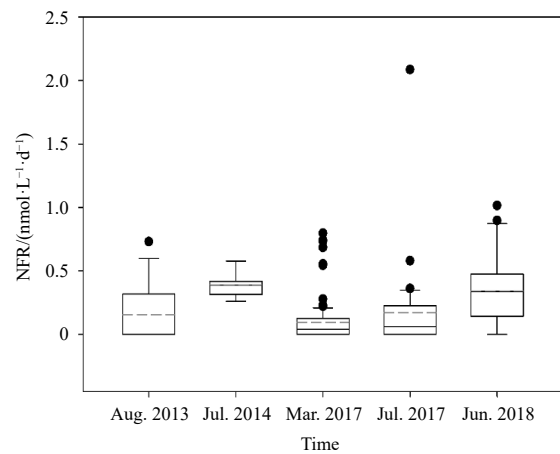


Fig. 2. The range of NFRs in the open area of the SCS (the top margins and the bottom margins of the boxes represent the third quartile (Q3) and the first quartile (Q1) respectively. The upper limit and the lower limit were calculated as follows: upper limit = $Q3 + (Q3 - Q1) \times 1.5$, lower limit = $Q1 - (Q3 - Q1) \times 1.5$. Values larger than the upper limit or less than the lower limit were defined as outliers. The solid lines in the boxes represent the medians, and the dotted lines represent the average values).

NFRs ranged from n.d. to 0.73 nmol/(L·d) ((0.15 ± 0.23) nmol/(L·d), $n=17$). In July 2014, surface NFRs ranged from 0.26 nmol/(L·d) to 0.58 nmol/(L·d) ((0.39 ± 0.10) nmol/(L·d), $n=7$), with higher NFRs observed at stations near Vietnam. In March 2017, surface NFRs ranged from n.d. to 0.80 nmol/(L·d) ((0.11 ± 0.16) nmol/(L·d), $n=24$), and the NFRs from 0 m to 150 m ranged from n.d. to 0.80 nmol/(L·d) ((0.16 ± 0.09) nmol/(L·d), $n=138$). The highest NFRs in March 2017 were observed at Station C-S27 (Fig. 3) and were obviously higher than those observed at other stations. In July 2017, surface NFRs ranged from n.d. to 0.36 nmol/(L·d) ((0.16 ± 0.14) nmol/(L·d), $n=7$), among which the surface NFRs at Stations G-N2

and G-F2 were higher than those of other stations. NFRs from 0–100 m ranged from n.d. to 2.08 nmol/(L·d) (0.17 ± 0.38 nmol/(L·d), $n=31$). In June 2018, surface NFRs ranged from 0.11 nmol/(L·d) to 0.90 nmol/(L·d) (0.43 ± 0.30 nmol/(L·d), $n=5$), with the highest NFR observed at the Station D-B3 and the lowest NFR at the Station D-D1 (Fig. 3a). NFRs at 0–150 m ranged from n.d. to 1.03 nmol/(L·d) (0.34 ± 0.27 nmol/(L·d), $n=29$). NFRs in the north-eastern SCS (near the Luzon Strait) and the sea areas east of Vietnam were generally higher than those in the other sampled areas (Fig. 3). At most sampling stations in this study, higher NFRs were generally observed in surface water, except for a few stations near Luzon Strait (such as Station G-N2), where the highest NFRs were observed at the subsurface.

NFRs in the Daya Bay ranged from n.d. to 4.51 nmol/(L·h), with higher NFRs observed in spring and summer (Li et al., 2019). The prominent feature of NFRs in the Daya Bay during the sampling period is that the NFRs were obviously higher than those in the neighboring open areas of the SCS.

3.2 Taxonomic composition of diazotrophs

A total of 26 000 high-quality reads based on *nifH* genetic fragments were obtained from the five stations during the cruise in March 2017 (see locations in Fig. 1a). The rarefaction curves reached plateaus, and the sequencing depth was sufficient to recover the diazotrophic communities. Cyanobacteria and proteobacterial *nifH* were the most abundant phylotypes in all samples, among which the cyanobacterial *nifH* was mainly composed of the unicellular cyanobacterium group A (UCYN-A) and *Trichodesmium*, and the proteobacteria *nifH* were mainly composed of Gammaproteobacteria and Alphaproteobacteria (Fig. 4). Except

for Station C-S1, Gammaproteobacteria were major contributors at all stations (>50% at Stations C-S41 and C-S57 and approximately 94% at 100 m of Station C-S59). Generally, the relative contribution of cyanobacteria decreased with depth, and the relative contribution of Gammaproteobacteria and Alphaproteobacteria increased. The fraction of cyanobacteria in the diazotrophic community at stations in the northern SCS (Stations C-S1, C-S6, and C-S25) were higher than those at the other stations.

3.3 Discrepancy of NFRs by using the B and S methods

A comparison of the NFRs measured by the B and S methods is shown in Fig. 5. In the southern SCS, NFRs observed by the B method (NFR-B) and S method (NFR-S) had significant difference (t test, $p < 0.05$, $n=17$ in August 2012, and $p < 0.01$, $n=7$ in July 2014). In August 2013, NFR-B and NFR-S ranged from n.d. to 0.78 nmol/(L·d) (0.21 ± 0.23 nmol/(L·d), $n=17$), and n.d. to 0.73 nmol/(L·d) (0.15 ± 0.24 nmol/(L·d), $n=17$), respectively, and the ratio of NFR-S/NFR-B (at the stations where both the NFR-B and NFR-S were both above the detection limit) ranged from 0.76 to 1.56 (1.09 ± 0.31 , $n=6$). In July 2014, NFR-B and NFR-S ranged from n.d. to 1.33 nmol/(L·d) (0.25 ± 0.48 nmol/(L·d), $n=7$) and 0.26 nmol/(L·d) to 0.58 nmol/(L·d) (0.39 ± 0.10 nmol/(L·d), $n=7$), respectively. Excluding the highest NFR observed by using the B method at Station K-C50 (1.33 nmol/(L·d)), NFR-S were obviously higher than NFR-B during this cruise (t test, $p < 0.01$, $n=6$), with NFR-S/NFR-B ranging between 0.29 and 4.37 (2.55 ± 1.76 , $n=3$).

The NFR-S/NFR-B ratio showed obvious seasonal variation in the Daya Bay (Fig. 5, excluding the bloom Station E-S4). During the summer cruise in July 2015, NFR-B and NFR-S ranged from

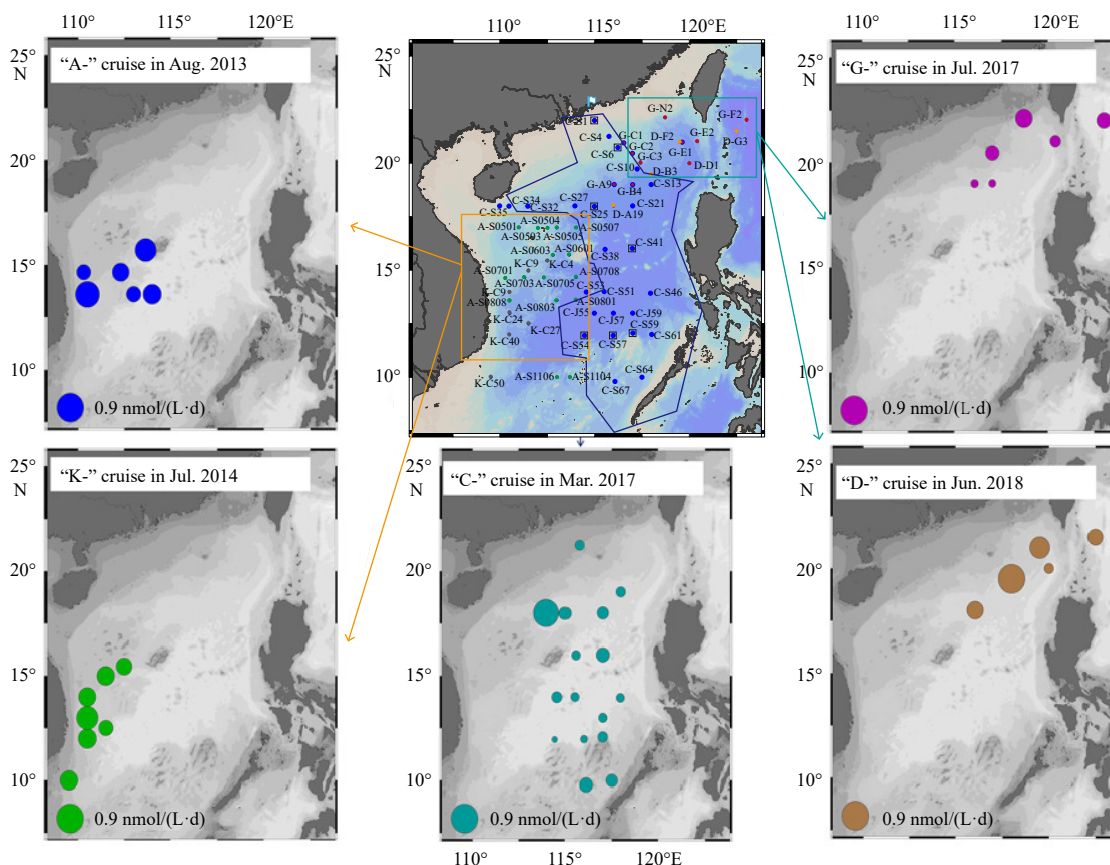


Fig. 3. Surface distribution of NFRs (nmol/(L·d)) in the open waters of the South China Sea (“A-”, “K-”, “C-”, “G-” and “D-” indicate cruises in August 2013, July 2014, March 2017, July 2017 and June 2018, respectively).

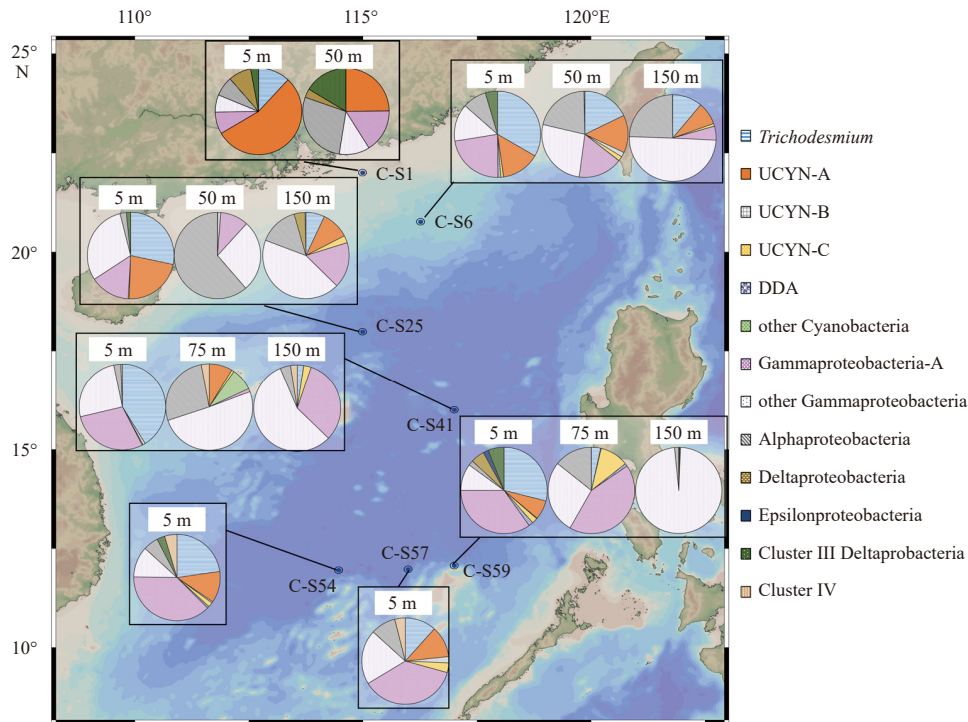


Fig. 4. Diazotrophic composition derived from *nifH* gene sequences in the open waters of South China Sea (March 2017). UCYN: unicellular cyanobacterium group; DDA: diatom diazotroph associations.

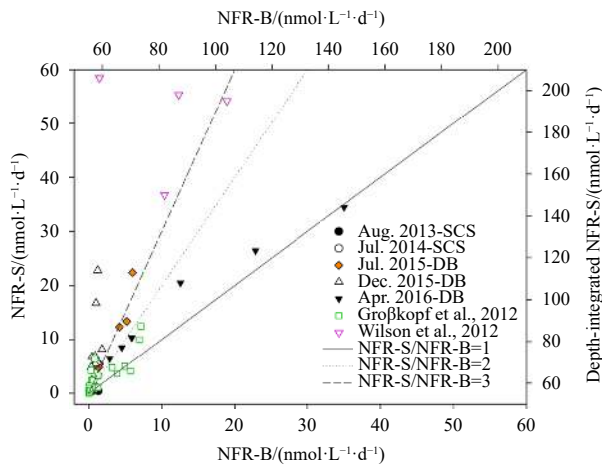


Fig. 5. The relationship between N_2 fixation rates (NFRs) measured by the original bubble (B) method and the $^{15}N_2$ -enriched seawater (S) methods: the unit of NFRs observed in this study and in Großkopf et al. (2012) is $nmol/(L \cdot d)$, and the unit of NFRs (depth-integrated NFRs) in Wilson et al. (2012) is $\mu mol/(m^2 \cdot d)$. To improve the visibility of Fig. 5, the unit of NFRs in the Daya Bay (DB) are converted to $nmol/(L \cdot d)$.

0.03 $nmol/(L \cdot h)$ to 0.94 $nmol/(L \cdot h)$ (0.03 $nmol/(L \cdot d)$ to 0.94 $nmol/(L \cdot d)$, $(5.97 \pm 7.62) nmol/(L \cdot d)$, $n=7$) and 0.06–4.51 $nmol/(L \cdot h)$ (1.53 $nmol/(L \cdot d)$ to 108.32 $nmol/(L \cdot d)$, $(24.02 \pm 37.82) nmol/(L \cdot d)$, $n=7$), with the max NFR observed at the bloomed Station E-S4. NFR-S was obviously higher than NFR-B (t test, $p < 0.01$, $n=9$), with NFR-S/NFR-B ratios ranging between 1.87 and 4.79 (3.27 ± 0.93 , $n=7$). In December 2015 (winter), NFRs in the Daya Bay were generally lower during, and NFR-S/NFR-B ratios were obviously higher than those in the spring and summer cruises (t test, $p < 0.01$, $n=10$).

NFR-B and NFR-S ranged from 0.01 $nmol/(L \cdot h)$ to 0.08 $nmol/(L \cdot h)$ (0.34 $nmol/(L \cdot d)$ to 1.81 $nmol/(L \cdot d)$, $(0.89 \pm 0.45) nmol/(L \cdot h)$, $n=10$) and 0.10–0.70 $nmol/(L \cdot h)$ (2.40 $nmol/(L \cdot d)$ to 22.80 $nmol/(L \cdot d)$, $(8.51 \pm 6.29) nmol/(L \cdot h)$, $n=10$), respectively, with NFR-S/NFR-B ranged from 4.50 to 18.53 (10.10 ± 5.36 , $n=10$). In spring (April 2016), the discrepancy between NFR-B and NFR-S was not significant (t test, $p > 0.05$, $n=9$). NFR-B and NFR-S ranged from 0.25 $nmol/(L \cdot h)$ to 1.46 $nmol/(L \cdot h)$ (2.88 $nmol/(L \cdot d)$ to 41.35 $nmol/(L \cdot d)$, $(17.87 \pm 15.52) nmol/(L \cdot h)$, $n=7$) and 0.27–1.43 $nmol/(L \cdot h)$ (6.43 $nmol/(L \cdot d)$ to 34.47 $nmol/(L \cdot d)$, $(17.71 \pm 10.26) nmol/(L \cdot h)$, $n=7$), respectively, while NFR-S/NFR-B ratio ranged from 0.98 to 2.23 (1.60 ± 0.46 , $n=7$).

3.4 Discrepancy of NFRs by using the B and MB methods

During the Daya Bay cruise in January 2018, NFR-MB and NFR-B ranged from 0.02 $nmol/(L \cdot h)$ to 4.06 $nmol/(L \cdot h)$ ($(0.45 \pm 1.10) nmol/(L \cdot h)$, $n=13$) and 0.01 $nmol/(L \cdot h)$ to 2.20 $nmol/(L \cdot h)$ ($(0.25 \pm 0.60) nmol/(L \cdot h)$, $n=13$), respectively. NFR-MB was obviously higher than NFR-B and had a significant linear correlation with NFR-B (t test, $p < 0.05$, $n=13$; Fig. 6a, with a slope of 1.8). Leaving aside the high NFR observed at Station E-S7 (NFR-MB = 4.06 $nmol/(L \cdot h)$, NFR-B = 2.20 $nmol/(L \cdot h)$), the slope of the linear equation in Fig. 6a is approximately 1.5. During the SCS cruise in June 2018, NFR-MB and NFR-B ranged from 0.07 $nmol/(L \cdot d)$ to 1.01 $nmol/(L \cdot d)$ ($(0.41 \pm 0.24) nmol/(L \cdot d)$, $n=24$) and 0.03 $nmol/(L \cdot d)$ to 0.41 $nmol/(L \cdot d)$ ($(0.16 \pm 0.11) nmol/(L \cdot d)$, $n=24$), respectively, with obvious discrepancy (t test, $p < 0.01$, $n=24$). A linear correlation between NFR-MB and NFR-B was also observed (Fig. 6b), with a slope of 1.9, which is similar to the slope observed in the Daya Bay. According to Fig. 6, the relationship between NFR-MB and NFR-B seems to be more stable than that between NFR-S and NFR-B, which has less variation by area. Although the incubation time, diazotrophic composition, and hydrological factors in the Daya Bay and the northeastern SCS have obvious differences,

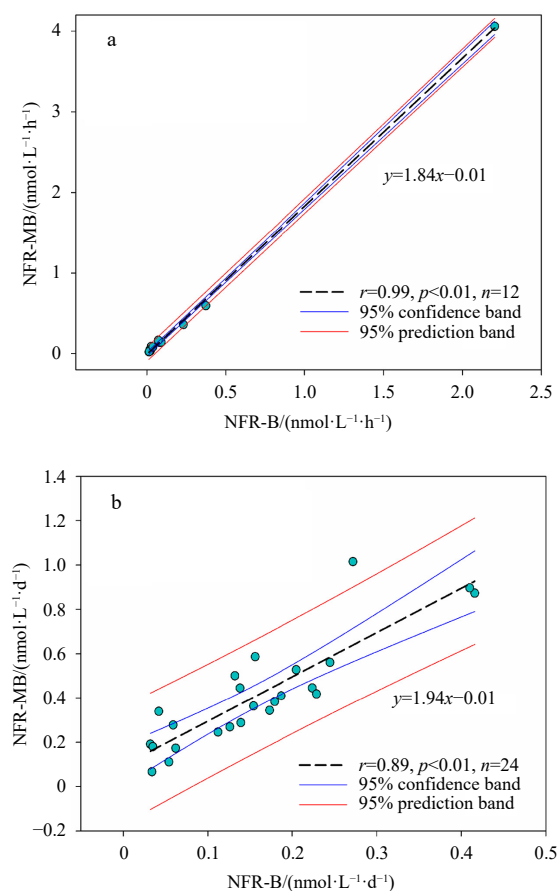


Fig. 6. The correlation between N_2 fixation rates measured by the original bubble (B) and modified bubble (MB) methods: a. the Daya Bay, January 2018; b. the northeastern SCS, June 2018.

the correlation between NFR-MB and NFR-B seems unaffected. This finding indicates that the comparison between NFR-MB and NFR-B may be more feasible for correcting the prior absolute majority of NFR datasets based on the B method.

4 Discussion

4.1 Toward a better understanding of the discrepancy between NFR-B and NFR-S

NFR-B and NFR-S observed in the open waters in this study generally fell in the range of published NFRs in the SCS (Table S1). Both the NFR-B and NFR-S in the Daya Bay were obviously higher than the earlier data of NFR in the open SCS.

The ratios of NFR-S/NFR-B observed in this study (0.76–4.37, 1.83 ± 1.27 , $n=9$ in the open SCS, 0.42–18.53, 5.58 ± 5.23 , $n=24$ in the Daya Bay) were also within the range reported in the literature. Großkopf et al. (2012) reported a large variation scale of NFR-S/NFR-B (0.53–42, 6.9 ± 9.2 , $n=25$) in the oligotrophic North Atlantic (Fig. 5). In contrast, the ratio observed at Station ALOHA in the North Pacific Subtropical Gyre appeared to fall in narrower ranges (NFR-S/NFR-B, ~ 1.8 to 3.5, Wilson et al., 2012; ~ 1.8 to 3.5, Böttjer et al., 2017). The obtained depth-integrated NFR based on S method in the open waters of the SCS (July 2017) averaged (22.36 ± 36.09) $\mu\text{mol}/(\text{m}^2 \cdot \text{d})$ ($n=31$, 0–200 m). However, the present understanding of average depth-integrated NFR of the SCS based on the B method was approximately $55 \mu\text{mol}/(\text{m}^2 \cdot \text{d})$ (Voss et al., 2006; Lin, 2013; Chen et al., 2014; Zhang et al., 2015; Liu et al., 2016, 2020; Wen et al., 2017; Li et al., 2019), which is ob-

viously higher than our result based on NFR-S. It seems to be contradictory to the average NFR-S/NFR-B in this study and the published literature (both >1). Thus, we propose that it may be risky to reevaluate the flux of N_2 fixation in the SCS solely based on the relationship between NFR-B and NFR-S, as the discrepancy between NFR-S and NFR-B may be complicated by other factors including the composition of diazotrophs and the length of incubation time.

Diazotrophic composition may be an important factor influencing the ratio of NFR-S/NFR-B. The analysis of *nifH* in March 2017 (Fig. 4), combined with the published literature (Bombar et al., 2010; Grosse et al., 2010; Ding et al., 2016), revealed the important contribution of *Trichodesmium* (Fig. 4) in the open area of SCS, indicating that the contribution of *Trichodesmium* to N_2 fixation can not be ignored here. However, *Trichodesmium* was not detected during our investigation in the Daya Bay. In this study, NFR-S/NFR-B in the Daya Bay was generally higher than that observed in the open areas of the SCS, indicating that dominance of *Trichodesmium* may lead to a lower NFR-S/NFR-B, which is similar to the results of Großkopf et al. (2012). Großkopf et al. (2012) observed an average NFR-S/NFR-B of 2.6 for the community-dominated *Trichodesmium*. For the diazotrophic community dominated by UCYN-A, diatom diazotroph associations, and proteobacteria, the ratios of NFR-S/NFR-B were higher (~ 6). This finding may be the result of the simultaneous incubation of floating *Trichodesmium* and the non-floating fraction. When NFRs were measured by the B method, the floating *Trichodesmium* was closer to the source of the tracer, the $^{15}\text{N}_2$ bubble, causing a smaller discrepancy between the NFR-S and NFR-B of *Trichodesmium* (Großkopf et al., 2012). The diurnal rhythm of N_2 fixation by diazotrophs may also influence NFR-S/NFR-B. Because a complete dissolution equilibration of $^{15}\text{N}_2$ gas generally takes longer than 12 h (Van Wambeke et al., 2018), the diazotrophic communities dominated by species fixing N_2 only during the daytime (such as UCYN-A) will probably be subject to a greater underestimation (Großkopf et al., 2012). The results in this study (Fig. 4) indicate a higher contribution of UCYN-A at Station C-S1, which located near the northern coast of the SCS. Our results in the Daya Bay also indicated the important contribution of UCYN-A (Li et al., 2019), especially at Station E-S11 ($\sim 96.6\%$), which may be one of the possible reason for the higher NFR-S/NFR-B in the Daya Bay. However, the understanding of the impact of diazotrophic composition on the discrepancy of NFRs measured by different methods is generally lacking, calling for further studies in the future.

The length of incubation time may be another important factor resulting in the discrepancy between NFR-B and NFR-S. For our sampling in August 2013 and July 2014 in the southern SCS, an incubation length of 24 h was adopted to be consistent with most of the published studies in open oceans (White et al., 2020); a shorter incubation duration (6 h) was adopted for the coastal cruises (the Daya Bay). The shorter duration is often used in the study of environmental settings, such as coastal and eutrophic waters. Because the equilibration degree of the injected $^{15}\text{N}_2$ gas bubble with seawater generally increases with time, a shorter incubation time may cause a larger discrepancy. Wannicke et al. (2018) found that a short incubation length (1 h) may cause a 30% underestimation of the $^{15}\text{N}_2$ concentration in the incubation system; they also found that a 12–24 h incubation may be sufficient for the equilibration between $^{15}\text{N}_2$ gas bubbles and surrounding water, which would have less influence on the discrepancy between NFR-B and NFR-S.

In addition to the composition of the diazotrophic community and incubation length, the spatiotemporally varying en-

vironmental parameters (i.e., water temperature, nutrient status, stratification, etc.) may also contribute to the discrepancy between NFR-S and NFR-B in the study area. Furthermore, the published results in the Atlantic and the fixed Station ALOHA in the North Pacific Subtropical Gyre (Böttjer et al., 2017; Großkopf et al., 2012; Wilson et al., 2012) may indicate that the discrepancy between NFR-B and NFR-S may be more influenced by the spatial variation of these factors, however, which need to be further tested in the future.

4.2 Re-evaluation of N_2 fixation flux in the SCS based on B and MB methods

It is fundamental to compare NFRs by using the B method for potentially fully use of available datasets of N_2 fixation and an improved understanding of the distribution pattern and controlling mechanism of this key biogeochemical process. There are two main reasons for this result. First, the majority of available marine NFR data are based on the B method (Großkopf et al., 2012; White et al., 2020). Second, the MB method may offer the most accurate field NFR that the science community can obtain using the $^{15}N_2$ tracer assay (Chang et al., 2019; Klawonn et al., 2015; White et al., 2020). When compared to the discrepancy between NFR-B and NFR-S, the relationship between NFR-B and NFR-MB is more stable, which seems not to be influenced by the large discrepancy of the diazotrophic composition, the incubation time and other environmental factors between the coastal Daya Bay and the open area of the SCS (Fig. 6). Hence, we suggest that the MB method may be the preferred method for NFR measurements and correction for three reasons: (1) MB methods can provide a higher and directly measured A_{N_2} , which may improve the availability of measured NFRs; (2) it can also avoid the preparation and preservation of the liquid tracer necessary for the S method and may minimize unprecedented contamination; (3) the correlation between NFR-MB and NFR-B is more stable, which seems to be more feasible for the correction of historical data based on the B method.

Our results suggest that earlier published data of NFRs based on the B method may have been underestimated by approximately 50%. This value is similar to the average result of Großkopf et al. (2012) and Böttjer et al. (2017). Based on the observed NFR-MB/NFR-B (approximately 2:1) in this study, the reevaluated average value of the depth-integrated NFRs in the SCS was elevated to be $110 \mu\text{mol}/(\text{m}^2\cdot\text{d})$ ($40 \text{ mmol}/(\text{m}^2\cdot\text{a})$). This value is within the range of our NFRs measured by the MB method (this study) in the northeastern SCS (June 2018, $49\text{--}114 \mu\text{mol}/(\text{m}^2\cdot\text{d})$, $(68\pm 16) \mu\text{mol}/(\text{m}^2\cdot\text{d})$, $n=5$). Our results may improve the availability and comparability of prior NFRs in the SCS. However, a large-scale comparison between the NFRs measured by the B, S, and MB methods is required in future research.

In addition to nitrogen fixation ($40 \text{ mmol}/(\text{m}^2\cdot\text{a})$), the source of new nitrogen in the euphotic layer of the SCS mainly includes the inputs of nitrate by deep water and atmospheric deposition, with an average flux of approximately $204 \text{ mmol}/(\text{m}^2\cdot\text{a})$ (Ren et al., 2017) and $49 \text{ mmol}/(\text{m}^2\cdot\text{a})$ (Kim et al., 2014), respectively. N_2 fixation accounts for approximately 20% of the total nitrogen input, similar to the nitrogen input from atmospheric deposition. Under a steady state, the export flux of nitrogen from the euphotic layer is approximately $293 \text{ mmol}/(\text{m}^2\cdot\text{a})$, which is within the range of the reported flux observed by sediment traps (Wong et al., 2007; Yang et al., 2017). However, the spatial-temporal variation of N_2 fixation may introduce uncertainty in the evaluation of N flux. Moreover, dissolved organic nitrogen may play a long overlooked role in N cycle in the SCS upper water column (Zhang et al., 2020).

5 Summary

In this study, we compared the divergent $^{15}N_2$ tracer assay for NFRs in the SCS, including the B method, S method, and MB method. Our results indicate that the discrepancy between NFRs measured by the B and S methods may vary obviously with area and season, which may be influenced by incubation time, diazotrophic composition, and hydrological factors. The correlation between NFRs measured by B and MB methods appears more reliable, indicating that the NFRs based on B methods may be undervalued by approximately 50%. Correcting the NFRs measured by the B method gave an average depth-integrated NFR of approximately $110 \mu\text{mol}/(\text{m}^2\cdot\text{d})$ (extrapolated annual rate $\sim 40 \text{ mmol}/(\text{m}^2\cdot\text{a})$), falling in the range of our field-measured depth-integrated NFRs by MB methods in the northeastern SCS. Our results provide implications for improving the validity of published NFRs in the SCS. Further validation of the $^{15}N_2$ tracer assay and the comparison of NFRs with respect to methodological difference are called for a more robust understanding of the distribution, controlling factors, and flux of N_2 fixation in the SCS and other oceanic regions as well.

Acknowledgements

We are grateful to the project team members for sampling assistance. Thanks are also due to scientists who kindly shared physical, chemical and biological data. Samples were collected during the open research cruises NORC2013-07, NORC2014-07, NORC2017-05, NORC2017-06 and NORC2018-05, supported by Natural Science Foundation of China Shiptime Sharing Project.

References

- Bombar D, Dippner J W, Doan H N, et al. 2010. Sources of new nitrogen in the Vietnamese upwelling region of the South China Sea. *Journal of Geophysical Research: Oceans*, 115(C6): C06018
- Bombar D, Paerl R W, Anderson R, et al. 2018. Filtration via conventional glass fiber filters in $^{15}N_2$ tracer assays fails to capture all nitrogen-fixing prokaryotes. *Frontiers in Marine Science*, 5: 6, doi: [10.3389/fmars.2018.00006](https://doi.org/10.3389/fmars.2018.00006)
- Böttjer D, Dore J E, Karl D M, et al. 2017. Temporal variability of nitrogen fixation and particulate nitrogen export at Station ALOHA. *Limnology and Oceanography*, 62(1): 200–216, doi: [10.1002/lno.10386](https://doi.org/10.1002/lno.10386)
- Casciotti K L. 2016. Nitrogen and oxygen isotopic studies of the marine nitrogen cycle. *Annual Review of Marine Science*, 8: 379–407, doi: [10.1146/annurev-marine-010213-135052](https://doi.org/10.1146/annurev-marine-010213-135052)
- Chang B X, Jayakumar A, Widner B, et al. 2019. Low rates of dinitrogen fixation in the eastern tropical South Pacific. *Limnology and Oceanography*, 64(5): 1913–1923, doi: [10.1002/lno.11159](https://doi.org/10.1002/lno.11159)
- Chen Yuh-Ling Lee, Chen Houng-Yung, Lin Yen-Huei, et al. 2014. The relative contributions of unicellular and filamentous diazotrophs to N_2 fixation in the South China Sea and the upstream Kuroshio. *Deep-Sea Research Part I: Oceanographic Research Papers*, 85: 56–71, doi: [10.1016/j.dsr.2013.11.006](https://doi.org/10.1016/j.dsr.2013.11.006)
- Chen Yuh-Ling Lee, Chen Houng-Yung, Tuo Sing-How, et al. 2008. Seasonal dynamics of new production from *Trichodesmium* N_2 fixation and nitrate uptake in the upstream Kuroshio and South China Sea Basin. *Limnology and Oceanography*, 53(5): 1705–1721, doi: [10.4319/lno.2008.53.5.1705](https://doi.org/10.4319/lno.2008.53.5.1705)
- Chen Shengbao, Zhang Run, Chen Nengwang, et al. 2018. On the introduction of $^{15}N_2$ tracer in marine N_2 fixation rate assay. *Haiyang Xuebao* (in Chinese), 40(10): 42–50
- Codispoti L A. 2007. An oceanic fixed nitrogen sink exceeding 400 Tg N a^{-1} vs the concept of homeostasis in the fixed-nitrogen inventory. *Biogeosciences*, 4(2): 233–253, doi: [10.5194/bg-4-233-2007](https://doi.org/10.5194/bg-4-233-2007)
- Dabundo R, Lehmann M F, Treibergs L, et al. 2014. The contamination of commercial $^{15}N_2$ gas stocks with ^{15}N -labeled nitrate and ammonium and consequences for nitrogen fixation measurements. *PLoS ONE*, 9(10): e110335, doi: [10.1371/journal.pone.0110335](https://doi.org/10.1371/journal.pone.0110335)
- Ding Changling, Sun Jun, Xue Bing. 2016. Winter and summer diazo-

- trophic cyanobacteria in the western South China Sea. *Haiyang Xuebao* (in Chinese), 38(4): 84–94
- Dugdale R C, Menzel D W, Ryther J H. 1961. Nitrogen fixation in the Sargasso Sea. *Deep-Sea Research*, 7(4): 297–300, doi: [10.1016/0146-6313\(61\)90051-X](https://doi.org/10.1016/0146-6313(61)90051-X)
- Gradoville M R, Bombar D, Crump B C, et al. 2017. Diversity and activity of nitrogen-fixing communities across ocean basins. *Limnology and Oceanography*, 62(5): 1895–1909, doi: [10.1002/lno.10542](https://doi.org/10.1002/lno.10542)
- Grosse J, Bombar D, Doan H N, et al. 2010. The Mekong River plume fuels nitrogen fixation and determines phytoplankton species distribution in the South China Sea during low and high discharge season. *Limnology and Oceanography*, 55(4): 1668–1680, doi: [10.4319/lo.2010.55.4.1668](https://doi.org/10.4319/lo.2010.55.4.1668)
- Großkopf T, Mohr W, Baustian T, et al. 2012. Doubling of marine dinitrogen-fixation rates based on direct measurements. *Nature*, 488(7411): 361–364, doi: [10.1038/nature11338](https://doi.org/10.1038/nature11338)
- Gruber N, Sarmiento J L. 1997. Global patterns of marine nitrogen fixation and denitrification. *Global Biogeochemical Cycles*, 11(2): 235–266, doi: [10.1029/97GB00077](https://doi.org/10.1029/97GB00077)
- Kim T W, Lee K, Duce R, et al. 2014. Impact of atmospheric nitrogen deposition on phytoplankton productivity in the South China Sea. *Geophysical Research Letters*, 41(9): 3156–3162, doi: [10.1002/2014GL059665](https://doi.org/10.1002/2014GL059665)
- Klawonn I, Lavik G, Böning P, et al. 2015. Simple approach for the preparation of $^{15}\text{N}_2$ -enriched water for nitrogen fixation assessments: evaluation, application and recommendations. *Frontiers in Microbiology*, 6: 769
- Kong Liangliang, Jing Hongmei, Kataoka T, et al. 2011. Phylogenetic diversity and spatio-temporal distribution of nitrogenase genes (*nifH*) in the northern South China Sea. *Aquatic Microbial Ecology*, 65(1): 15–27, doi: [10.3354/ame01531](https://doi.org/10.3354/ame01531)
- Li Danyang, Liu Jiaxing, Zhang Run, et al. 2019. N_2 fixation impacted by carbon fixation via dissolved organic carbon in the changing Daya Bay, South China Sea. *Science of the Total Environment*, 674: 592–602, doi: [10.1016/j.scitotenv.2019.04.176](https://doi.org/10.1016/j.scitotenv.2019.04.176)
- Li Danyang, Zhang Run. 2018. Research progresses in biological nitrogen fixation in the South China Sea. *Journal of Xiamen University: Natural Science* (in Chinese), 57(6): 760–767
- Lin Feng. 2013. Spatial and temporal variations of biological N_2 fixation rate and its controlling factors in the China marginal seas (in Chinese) [dissertation]. Xiamen: Xiamen University
- Liu Jiaxing, Zhou Linbin, Li Gang, et al. 2016. Nitrogen fixation and its contribution of nitrogen to primary production in the surface waters of the northeastern South China Sea during October 2014. *Journal of Tropical Oceanography* (in Chinese), 35(5): 38–47
- Liu Jiaxing, Zhou Linbin, Li Jiajun, et al. 2020. Effect of mesoscale eddies on diazotroph community structure and nitrogen fixation rates in the South China Sea. *Regional Studies in Marine Science*, 35: 101106, doi: [10.1016/j.rsma.2020.101106](https://doi.org/10.1016/j.rsma.2020.101106)
- Mohr W, Großkopf T, Wallace D W R, et al. 2010. Methodological underestimation of oceanic nitrogen fixation Rates. *PLoS ONE*, 5(9): e12583, doi: [10.1371/journal.pone.0012583](https://doi.org/10.1371/journal.pone.0012583)
- Montoya J P, Voss M, Kahler P, et al. 1996. A simple, high-precision, high-sensitivity tracer assay for N_2 fixation. *Applied and Environmental Microbiology*, 62(3): 986–993, doi: [10.1128/aem.62.3.986-993.1996](https://doi.org/10.1128/aem.62.3.986-993.1996)
- Osorio-Santos K, Pietrasiak N, Bohunická M, et al. 2014. Seven new species of *Oculatella* (*Pseudanabaenales*, *Cyanobacteria*): taxonomically recognizing cryptic diversification. *European Journal of Phycology*, 49(4): 450–470, doi: [10.1080/09670262.2014.976843](https://doi.org/10.1080/09670262.2014.976843)
- Ren Haojia, Chen Yi-Chi, Wang Xingchen T, et al. 2017. 21st-century rise in anthropogenic nitrogen deposition on a remote coral reef. *Science*, 356(6339): 749–752, doi: [10.1126/science.aal3869](https://doi.org/10.1126/science.aal3869)
- Schloss P D. 2009. A high-throughput DNA sequence aligner for microbial ecology studies. *PLoS ONE*, 4(12): e8230, doi: [10.1371/journal.pone.0008230](https://doi.org/10.1371/journal.pone.0008230)
- Shiozaki T, Chen Yuh-Ling Lee, Lin Yen-Huei, et al. 2014. Seasonal variations of unicellular diazotroph groups A and B, and *Trichodesmium* in the northern South China Sea and neighboring upstream Kuroshio Current. *Continental Shelf Research*, 80: 20–31, doi: [10.1016/j.csr.2014.02.015](https://doi.org/10.1016/j.csr.2014.02.015)
- Van Wambeke F, Gimenez A, Duhamel S, et al. 2018. Dynamics and controls of heterotrophic prokaryotic production in the western tropical South Pacific Ocean: links with diazotrophic and photosynthetic activity. *Biogeosciences*, 15(9): 2669–2689, doi: [10.5194/bg-15-2669-2018](https://doi.org/10.5194/bg-15-2669-2018)
- Voss M, Bombar D, Loick N, et al. 2006. Riverine influence on nitrogen fixation in the upwelling region off Vietnam, South China Sea. *Geophysical Research Letters*, 33(7): L07604
- Wannicke N, Benavides M, Dalsgaard T, et al. 2018. New perspectives on nitrogen fixation measurements using $^{15}\text{N}_2$ gas. *Frontiers in Marine Science*, 5: 120, doi: [10.3389/fmars.2018.00120](https://doi.org/10.3389/fmars.2018.00120)
- Wen Zuozhu, Lin Wenfang, Shen Rong, et al. 2017. Nitrogen fixation in two coastal upwelling regions of the Taiwan Strait. *Scientific Reports*, 7(1): 17601, doi: [10.1038/s41598-017-18006-5](https://doi.org/10.1038/s41598-017-18006-5)
- White A E, Granger J, Selden C, et al. 2020. A critical review of the $^{15}\text{N}_2$ tracer method to measure diazotrophic production in pelagic ecosystems. *Limnology and Oceanography: Methods*, 18(4): 129–147, doi: [10.1002/lom3.10353](https://doi.org/10.1002/lom3.10353)
- Wilson S T, Böttjer D, Church M J, et al. 2012. Comparative assessment of nitrogen fixation methodologies, conducted in the oligotrophic North Pacific Ocean. *Applied and Environmental Microbiology*, 78(18): 6516–6523, doi: [10.1128/AEM.01146-12](https://doi.org/10.1128/AEM.01146-12)
- Wong George T F, Tseng Chun-Mao, Wen Liang-Saw, et al. 2007. Nutrient dynamics and N-anomaly at the SEATS station. *Deep-Sea Research Part II: Topical Studies in Oceanography*, 54(14–15): 1528–1545
- Yang Jin-Yu Terence, Kao Shui-Ji, Dai Minhan, et al. 2017. Examining N cycling in the northern South China Sea from N isotopic signals in nitrate and particulate phases. *Journal of Geophysical Research: Biogeosciences*, 122(8): 2188–2136
- Zehr J P, Capone D G. 2020. Changing perspectives in marine nitrogen fixation. *Science*, 368(6492): eaay9514, doi: [10.1126/science.aay9514](https://doi.org/10.1126/science.aay9514)
- Zehr J P, Montoya J P, Jenkins B D, et al. 2007. Experiments linking nitrogenase gene expression to nitrogen fixation in the North Pacific subtropical gyre. *Limnology and Oceanography*, 52(1): 169–183, doi: [10.4319/lo.2007.52.1.0169](https://doi.org/10.4319/lo.2007.52.1.0169)
- Zehr J P, Turner P J. 2001. Nitrogen fixation: Nitrogenase genes and gene expression. *Methods in Microbiology*, 30: 271–286
- Zhang Run, Chen Min, Yang Qing, et al. 2015. Physical-biological coupling of N_2 fixation in the northwestern South China Sea coastal upwelling during summer. *Limnology and Oceanography*, 60(4): 1411–1425, doi: [10.1002/lno.10111](https://doi.org/10.1002/lno.10111)
- Zhang Run, Wang Xingchen T, Ren Haojia, et al. 2020. Dissolved organic nitrogen cycling in the South China Sea from an isotopic perspective. *Global Biogeochemical Cycles*, 34(12): e2020GB006551
- Zhang Run, Zhang Dongsheng, Chen Min, et al. 2019. N_2 fixation rate and diazotroph community structure in the western tropical North Pacific Ocean. *Acta Oceanologica Sinica*, 38(12): 26–34, doi: [10.1007/s13131-019-1513-4](https://doi.org/10.1007/s13131-019-1513-4)

Supplementary information:

Table S1. Earlier data of N_2 fixation rates measured in the South China Sea.

The supplementary information is available online at <https://doi.org/10.1007/s13131-022-2092-3> and <http://www.aosocean.com/>. The supplementary information is published as submitted, without typesetting or editing. The responsibility for scientific accuracy and content remains entirely with the authors.